3 Biotech (2018) 8:404
https://doi.org/10.1007/s13205-018-1420-y

ORIGINAL ARTICLE

Biofabricated silver nanoparticles incorporated polymethyl methacrylate as a dental adhesive material with antibacterial and antibiofilm activity against *Streptococcus mutans*

Roshmi Thomas[1] · S. Snigdha[2] · K. B. Bhavitha[2,3] · Seethal Babu[1] · Anjitha Ajith[1] · E. K. Radhakrishnan[1]

Received: 21 May 2018 / Accepted: 1 September 2018 / Published online: 10 September 2018

Abstract

In this study, polymethyl methacrylate (PMMA) thin films incorporated with biofabricated silver nanoparticles were used to evaluate the in vitro antimicrobial and antibiofilm activity against the cariogenic bacterium *Streptococcus mutans*. For this, silver nanoparticles (AgNPs) were generated using *Bacillus amyloliquefaciens* SJ14 culture (MAgNPs) and extract from *Curcuma aromatica* rhizome (CAgNPs). The AgNPs were further characterized by UV–Vis spectroscopy and high-resolution transmission electron microscopy. The minimum inhibitory concentration, minimum bactericidal concentration and antibiofilm activity of AgNPs against *S. mutans* were also assessed. Here, MAgNPs were found to have superior antimicrobial activity when compared to CAgNPs. The MAgNPs and CAgNPs also demonstrated 99% and 94% inhibition of biofilm formation of *S. mutans* at concentrations of 3 µg/mL and 50 µg/mL, respectively. The AgNPs were further incorporated into PMMA thin films using solvent casting method. The thin films were also characterized by scanning electron microscopy and UV–Vis spectroscopy. Subsequently, both PMMA/MAgNPs and PMMA/CAgNPs nanocomposite thin films were subjected to antimicrobial and antibiofilm analysis. The microbicidal activity was found to be higher for the PMMA/MAgNPs thin film, which highlights the potency of microbially synthesized AgNPs as excellent agents to inhibit cariogenic bacteria from colonising dental restorative material.

Keywords Microbial AgNPs · Biofabricated AgNPs · Antibiofilm · Dental adhesive · PMMA · *Streptococcus mutans*

Introduction

Dental restorative composites mainly consist of methacrylate resins and various kinds of fillers which enhance their mechanical, antimicrobial, optical and aesthetic properties (Babu et al. 2016; Dionysopoulos et al. 2017). Dental adhesives facilitate the binding of composites to the dentin and form an interlocked interface by penetrating into the dentin tubules. Polymethyl methacrylate (PMMA), a transparent thermoplastic has been widely used as a constituent of dental material (Takeyama et al. 1978). Its acceptance in dentistry is due to its reliability, biocompatibility, low cost, easy availability, and the ease of modification (Frazer et al. 2005; Peters et al. 2018; Lee et al. 2018). However, one of the challenges with its application is the microbial biofilm formation at the dentin–adhesive interface leading to the failure of dental restoratives (Marashdeh et al. 2018).The biofilm formation in the oral cavity is generally favored by the presence of moisture and nutrients (Saini et al. 2011; Dias et al. 2017). Due to this, cariogenic bacteria like *Streptococcus mutans* forms one of the major culprits responsible for the failure of dental restorative material. The organism has been known to have preference to grow both on tooth surfaces and on surfaces of dental implant (Loesche 1986). There is high demand to develop engineered dental restorative materials with antimicrobial potential because of the increasing antibiotic resistance among these microorganisms (Garcia et al. 2017).

Roshmi Thomas and S. Snigdha contributed equally.

✉ E. K. Radhakrishnan
radhakrishnanek@mgu.ac.in

[1] School of Biosciences, Mahatma Gandhi University, PD Hills (P.O.), Kottayam, Kerala 686 560, India

[2] International and Inter University Centre for Nanoscience and Nanotechnology, Mahatma Gandhi University, PD Hills (P.O.), Kottayam, Kerala 686 560, India

[3] Department of Physics, St Teresas's College, Ernakulam, Kerala 682011, India

Among the diverse antimicrobials, silver has been widely considered to have low toxicity to humans and broad spectrum antagonistic effect on pathogenic microbes (Clement and Jarrett 1994). Especially in the past few decades, silver in the form of silver nanoparticles (AgNPs) has gained widespread acceptance as a promising antimicrobial, due to its enhanced nano-based properties. Due to this, many AgNPs based consumer products are available in the market. Silver nanoparticles (AgNPs) are synthesized extensively by chemical, physical and biological methods. Eventhough some studies indicate the concern with oxidative stress and associated complications for chemically synthesized silver ions (Srivastava et al. 2012), generally the effect can be concentration dependent. Hopefully, the biologically synthesized nanoparticles which are capped with bio-molecules of microbial or plant origin can be considered to have less toxic effects. The green synthesis methods involve the use of ecofriendly reductants and capping agents such as proteins, peptides, carbohydrates, plant extract, bacteria, fungi and algae. The relative ease with genetic and cultural manipulations make the bacterial system attractive for enhanced nanoparticle synthesis (Parikh et al. 2008, 2011). Mainly the peptides and carbohydrates present in biomaterials have been demonstrated to have stabilizing effect on the synthesized nanoparticle. These bio-based AgNPs are particularly attractive owing to their higher stability, lower toxicity, and ease with which biomaterials can be handled and manipulated for nanoparticles synthesis (Ge et al. 2014; Saifuddin et al. 2009).

Considering the advantages of the biofabricated AgNPs, current study was designed to compare and evaluate the microbicidal properties of AgNPs prepared by two biogenic routes to explore their application against *S. mutans*. For this, the antimicrobial and antibiofilm properties of AgNPs prepared using *Curcuma aromatica* extract and *Bacillus amyloliquefaciens* SJ14 culture were initially analyzed. Then these AgNPs were immobilized into PMMA matrix to study their in vitro effectiveness against *S. mutans*. The results of the study showed superior efficiency of microbially synthesized AgNPs over the phytoformulated AgNPs to act against *S. mutans*. Many previous studies have already reported the efficiency, stability and enhanced activity of microbially synthesized NPs when compared to those prepared by chemical methods (Saifuddin et al. 2009; Antony et al. 2011; Thomas et al. 2017). However, the current results indicate the need to explore diverse biogenic AgNPs to identify the one with optimal performance. Here, microbially generated AgNPs (MAgNPs) were found to have enhanced effectiveness to manage *S. mutans*, a common dental pathogen.

Materials and methods

Biosynthesis of AgNPs using bacteria and *Curcuma aromatica* rhizome extract

For the bacterial synthesis of silver nanoparticles, *B. amyloliquefaciens* SJ14 which was characterized previously for AgNPs synthesis by our group (Das et al. 2014), was selected. The bacterial strain was obtained from heavy metal contaminated area in Kochi, Kerala, India. For the AgNP synthesis, the bacterial isolate was inoculated into 100 mL nutrient broth (0.5% peptone, 0.15% beef extract, 0.15% yeast extract and 1% NaCl, pH 7) and the biomass was collected by centrifugation at 10,000 rpm after incubation at room temperature for 24 h in a rotating shaker set at 200 rpm. For the synthesis of AgNPs, about 2 g of bacterial wet biomass was mixed with 100 mL aqueous solution of filter sterilized 1 mM $AgNO_3$ and kept under visible light (Thomas et al. 2015). The AgNPs (MAgNPs) formed were purified and then characterized using UV–Vis spectroscopy (Shimadzu UV 2600 Spectrophotometer) and high-resolution transmission electron microscopy (JEOL 2100-HRTEM).

For the biosynthesis of AgNPs using *C. aromatica* rhizome, the plant material was purchased from Indian Institute of Spices Research (IISR), Kozhikode, Kerala, India. The rhizomes were washed to remove the adhering mud particles and impurities. 20 g of the rhizome was cut into small pieces and pulverized with a mortar and pestle. The ground material was squeezed through muslin cloth and was filtered using Whatmann No. 1 filter paper. For AgNPs synthesis, 45 mL of Milli-Q Ultrapure water was mixed with 5 mL of *C. aromatica* rhizome extract and $AgNO_3$ at a final concentration of 1 mM. This mixture was then incubated in the presence of fluorescent light. The extract without $AgNO_3$ was also maintained under similar conditions as control (Shameli et al. 2012; Velmurugan et al. 2014). The AgNPs (CAgNPs) formed were purified and characterized as described above.

Antibacterial activity of AgNPs against *Streptococcus mutans*

Minimum inhibitory concentration (MIC) by Resazurin-based 96-well plate microdilution method

The minimum inhibitory concentration (MIC) of synthesized AgNPs was analyzed by micro-broth dilution method as per the guidelines of the Clinical Laboratory Standards Institute (CLSI) using 96-well microtiter plates. The bacterial pathogen *S. mutans* (MTCC 497) was cultured in Brain

Heart Infusion (BHI) broth at 37 °C. The overnight culture was further diluted with BHI broth to obtain a bacterial cell density of 10^8 CFU/mL or 0.5 McFarland standard. The MIC of AgNPs against *S. mutans* was determined in BHI broth using serial twofold dilutions of AgNPs in a concentration range of 250–0.48 µg/mL. Growth and sterility control wells were also maintained in the micro titer plate. After the incubation at 37 °C for 24 h, 30 µL of resazurin (0.015%) was added to all the wells and incubated for 2–4 h. The wells with no color change (blue resazurin color remained unchanged) were scored as above MIC value. The assays were performed in triplicates to confirm the value of MIC of AgNPs against *S. mutans* (Elshikh et al. 2016).

Minimum bactericidal concentration (MBC)

The minimum bactericidal concentration (MBC) was determined by spread plating *S. mutans* (MTCC 497) culture from the wells with concentrations higher than the MIC value on the BHI agar plates followed by incubation at 37 °C for 24 h. The concentration at which the bacteria were completely killed was considered as MBC (Araruna et al. 2013).

Antibiofilm activity of AgNPs against *Streptococcus mutans*

The antibiofilm potential of both MAgNPs and CAgNPs against *S. mutans* was analyzed by tissue culture plate (TCP) method. Here, the organism was inoculated into BHI medium and incubated at 37 °C for 24 h. The cultures were then serially diluted to 1:100 in fresh liquid medium in a 96-well polystyrene microtiter plate. This was further treated with five different concentrations of AgNPs (100–6.25 µg/mL) followed by incubation at 37 °C for 24 h. After this, the unattached cells were removed, and the wells were washed twice with phosphate buffer saline (PBS). The attached cells were further stained with 0.1% crystal violet for 20 min. Excess stain was removed by thorough washing with de-ionised water and the plate was air dried. For the quantification of antibiofilm activity of AgNPs, the adherent bacteria associated with crystal violet were solubilized with 95% ethanol, and the absorbance were recorded at 590 nm using microplate reader (Thermo scientific Varioskan Flash Multimode reader). The obtained optical density (OD) value was considered as an index of bacterial ability to adhere to the surface and thereby facilitate biofilm formation as per the following equation (Christensen et al. 1985).

$$\frac{N_{\text{Sample}}}{V_{\text{Sample}}} \sim \text{OD}, \tag{1}$$

where $\frac{N_{\text{Sample}}}{V_{\text{Sample}}}$ is the cell number per unit volume, N_{sample} is the cell number in growth media of volume V (V_{sample}). From the OD values, the percentage of biofilm inhibition was calculated by the following formula

$$\%\ \text{of inhibition} = \frac{\text{OD control} - \text{OD treated}}{\text{OD control}} \times 100. \tag{2}$$

This assay was performed in triplicates. The average value and the standard deviation of the data were calculated and were compared using the Tukey test. A p value less than 0.05 was considered statistically significant.

Preparation of PMMA membranes

Poly (methyl methacrylate) powder purchased from Sigma-Aldrich (Mw ~ 1,20,000, d 1.188 g/mL at 25 °C) was dissolved in chloroform at a 14 wt% concentration by mechanical stirring for 6 h. This solution was then casted onto glass Petri dishes and allowed to dry at room temperature overnight. The dried membrane was peeled for further characterization studies. For the preparation of PMMA/MAgNP membrane, 3.5% of MAgNPs were added into the PMMA solution, stirred for 6 h, casted onto glass Petri dish and dried at room temperature overnight. Likewise PMMA/CAgNP membrane was prepared using 3.5% of CAgNPs.

Surface morphology of membranes

The surface features of the fabricated membranes were analyzed using scanning electron microscopy (SEM). The neat PMMA and PMMA/AgNP nanocomposite membranes were carefully sectioned into 3 × 0.5 mm pieces and were mounted on specimen stubs. These were coated with platinum in a sputter coater and examined under JEOL 6390 SEM JSM at 10 kV.

UV–Vis spectroscopy

The prepared membranes were also characterized using UV–Vis spectrophotometer (Agilent Cary 5000) as described earlier (Mathew et al. 2018).

Antibacterial activity against *Streptococcus mutans*

The antibacterial activity of developed PMMA/AgNP nanocomposites was evaluated against *S. mutans* by standard disc diffusion method using BHI agar plates. For this, *S. mutans* was cultured in brain heart infusion (BHI) broth at 37 °C for 24 h. This was followed by diluting the bacterial culture in BHI broth to get a culture density equivalent to a 0.5 McFarland standard. The culture was then swabbed uniformly onto the individual plates using sterile cotton swabs to create a

confluent lawn of bacterial growth. The discs of developed membranes along with controls were cut into 6 mm diameter pieces and were placed aseptically on the surface of the inoculated BHI agar plates. After incubation at 37 °C for 24 h, the zone of inhibition in millimeters around each disc was measured and the assays were implemented in triplicates.

Antibiofilm potential analysis of PMMA/AgNPs membranes by scanning electron microscopy

The efficacy of developed membranes to inhibit the biofilm formation by *S. mutans* was examined by SEM analysis. The neat PMMA and AgNPs incorporated PMMA membrane discs were aseptically introduced into BHI broth, inoculated with *S. mutans* and incubated at 37 °C for 48 h. The culture samples were then fixed in a solution of 2.5% glutaraldehyde prepared in 0.1 M sodium phosphate buffer (pH 7.3) for 2 h followed by wash with 0.1 M sodium phosphate buffer (pH 7.3). Samples were further dehydrated by passing through 30%, 50%, and 80% and 100% ethanol each for 10 min. Dried samples were then coated with platinum in a sputter coater and examined under JEOL 6390 SEM JSM at 20 kV in different magnifications (Agarwala et al. 2014).

Results

Characterization of biologically synthesized silver nanoparticles

On carrying out the UV–Vis absorption measurement, both the biogenic silver nanoparticles (CAgNPs and MAgNPs) were found to have characteristic absorption peak at 420 nm (Fig. 1) (Shameli et al. 2012; Quaresma et al. 2009).

Characterization of microbially synthesized silver nanoparticles (MAgNPs)

From the TEM micrographs, MAgNPs were observed to be associated with microbial remnants. These also revealed the irregular shapes of the nanoparticles with majority having a size range of 10–30 nm (Fig. 2).

Characterization of *Curcuma aromatic* extract fabricated modified silver nanoparticles (CAgNPs)

The CAgNPs were appeared to be dispersed in a matrix of plant extract as observed in the TEM images. The nanoparticle populations were predominantly circular with rods and triangles dispersed in between. More than 50% of the nanoparticles were observed to have diameters ranging from 20 to 40 nm (Fig. 3).

The MIC and MBC analysis (Table 1) showed the MAgNPs to have twofold higher efficiency when compared to CAgNPs in their antimicrobial properties. Only 3.9 µg/mL of MAgNPs was required to inhibit *S. mutans* when compared to the 7.8 µg/mL of CAgNPs required to achieve the same. Similarly, MAgNPs exhibited bactericidal activity at a concentration of 62.5 µg/mL, whereas 125 µg/mL of CAgNPs was required for killing *S. mutans*.

Comparative antibiofilm activity of two types of AgNPs (Fig. 4) showed excellent antibiofilm properties of AgNPs. At 50 µg/mL concentration, MAgNPs showed 99% inhibition and CAgNPs showed 94% inhibition (Fig. 4).

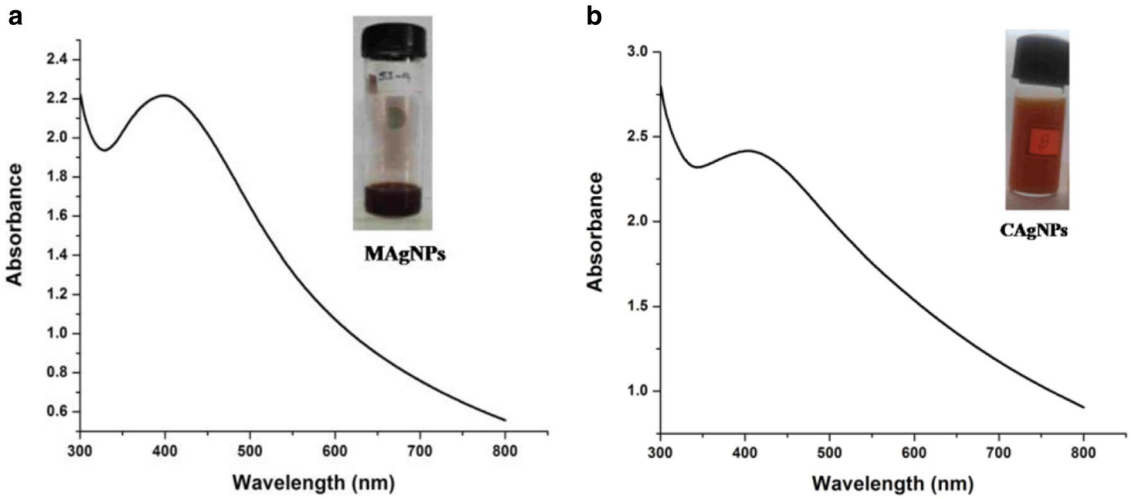

Fig. 1 **a** Visual observation and UV–Vis absorption spectrum of silver nanoparticles synthesized by **a** *Bacillus amyloliquefaciens* SJ14, inset: photograph of MAgNP solution and **b** *Curcuma aromatica* rhizome extract, inset: photograph of CAgNP solution

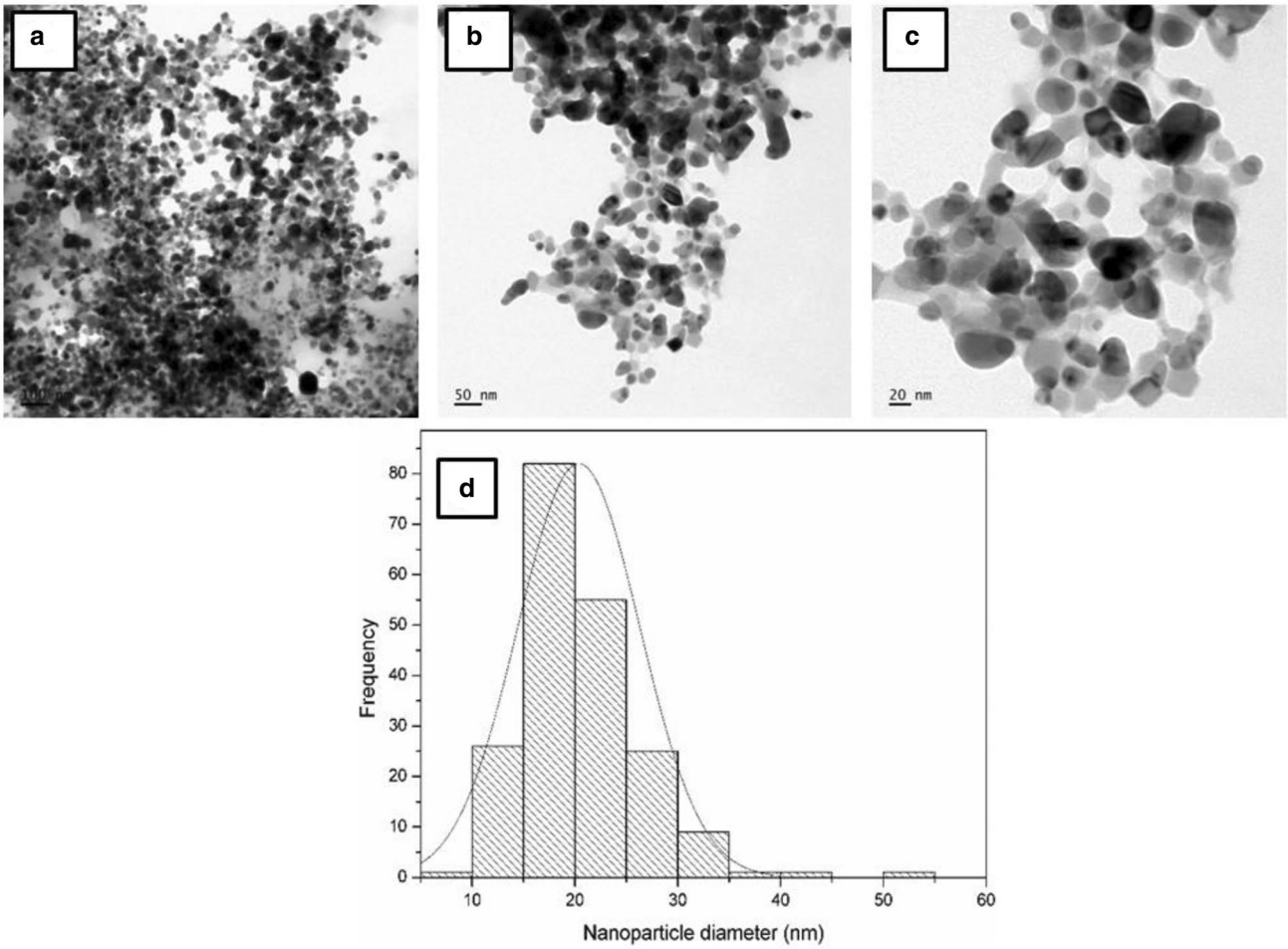

Fig. 2 High-resolution transmission electron micrographs (**a**–**c**) and size distribution of nanoparticles (**d**) of AgNPs synthesized by *Bacillus amyloliquefaciens* SJ14. Scale bar for **a** is 100 nm, **b** is 50 nm and **c** is 20 nm

The neat PMMA membrane exhibited solvent evaporation-induced circular blind pores of approximately 5–10 µm diameter. The pores were observed throughout the surface of the membrane and the areas surrounding the pores appeared smooth. However, upon addition of the filler, the numbers of pores were drastically reduced and the surface showed large pores. The surface of the membrane and the areas surrounding the large pores appeared to be surrounded by white aggregates, which could be the AgNPs incorporated in the membrane (Fig. 5). The majority of the MAgNPs appeared to be surrounding the pores of PMMA and the CAgNPs were found to be accumulated in the cavity of the pores (Qian et al. 2010).

The incorporation of MAgNPs and CAgNPs in the PMMA matrix was also confirmed by UV–Vis spectroscopy. The UV–Vis spectra (Fig. 6), showed the SPR peak of AgNPs embedded in the PMMA matrix. The absorption peaks of both the nanoparticles were found to be broadened upon incorporation into the PMMA matrix (Mei et al. 2014).

The membranes were examined for antimicrobial activity against *S. mutans*, a common pathogen of the oral cavity. After 24 h incubation, the CAgNPs incorporated PMMA membrane exhibited less activity against the test organism, whereas the MAgNPs exhibited significant antimicrobial activity as indicated by a zone of inhibition of 12 mm (Fig. 7).

The antibiofilm properties of the membrane incorporated NPs were evident from the SEM micrographs (Fig. 8). The neat PMMA membrane harbored microbial biofilms which can be clearly observed in Fig. 8a–c. The well-developed bacterial biofilm colonies can be observed in Fig. 8c. Both the nanocomposite membranes significantly hindered the growth and biofilm forming ability of the *S. mutans*.

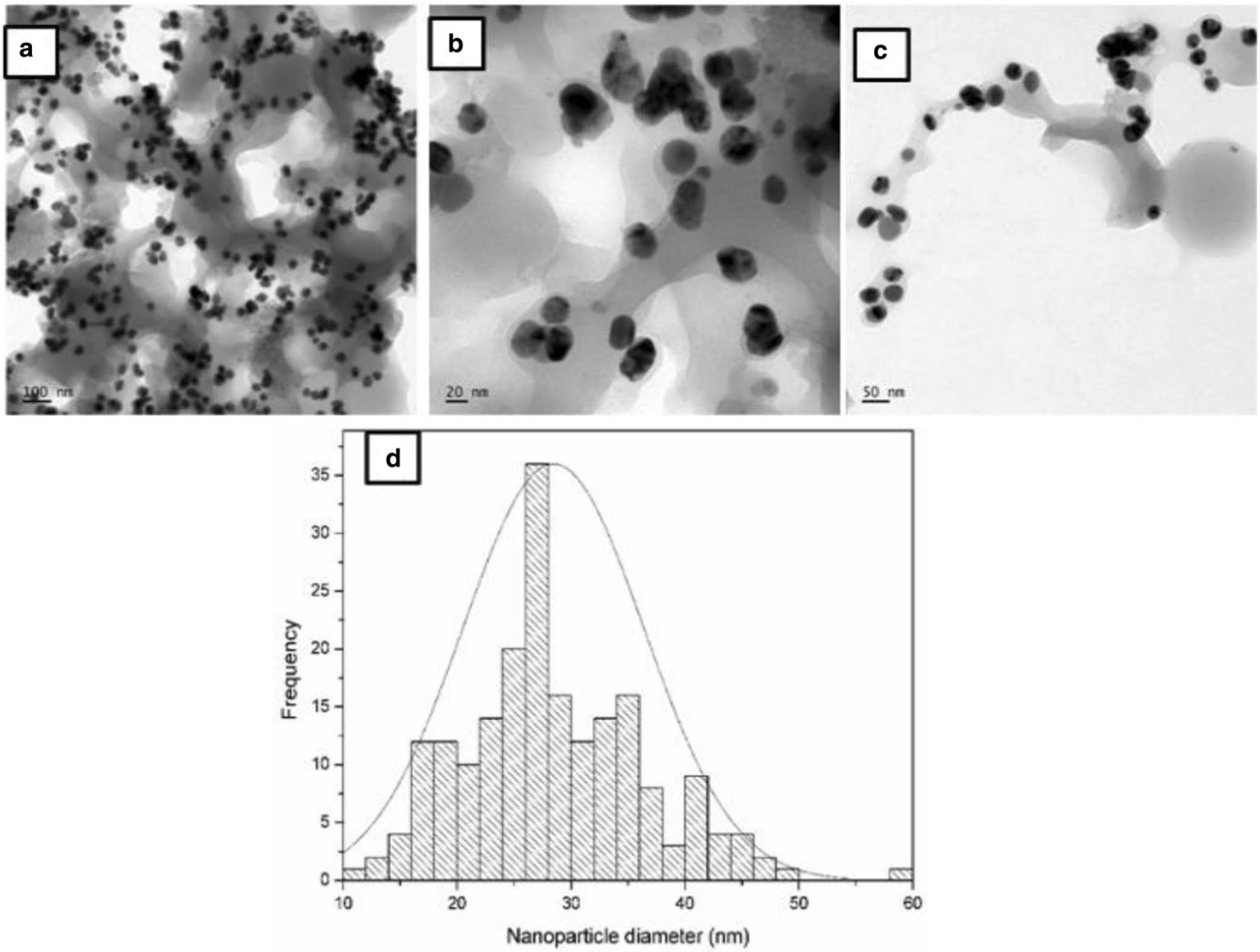

Fig. 3 High-resolution transmission electron microscopic images (**a**–**c**) and size distribution of nanoparticles (**d**) of AgNPs synthesized by extract from *Curcuma aromatica* rhizome. Scale bar for Fig. 2a is 100 nm, Fig. 2b is 50 nm and Fig. 2c is 20 nm

Table 1 Minimum inhibitory concentration (MIC) and minimum bactericidal concentration (MBC) of biosynthesized AgNPs (µg/mL) against *Streptococcus mutans, n* = 6

Samples	MIC (µg/mL)	MBC (µg/mL)
MAgNPs	3.9	62.5
CAgNPs	7.8	125

Discussion

Engineering of dental restorative composites for antimicrobial properties is of great interest due to increasing reports on plaque formation, which can be attributed primarily due to bacterial biofilm and its associated debris. Hence in this study, antimicrobial and antibiofilm properties of biofabricated AgNPs embedded polymethyl methacrylate (PMMA) were analyzed. The UV–Vis and

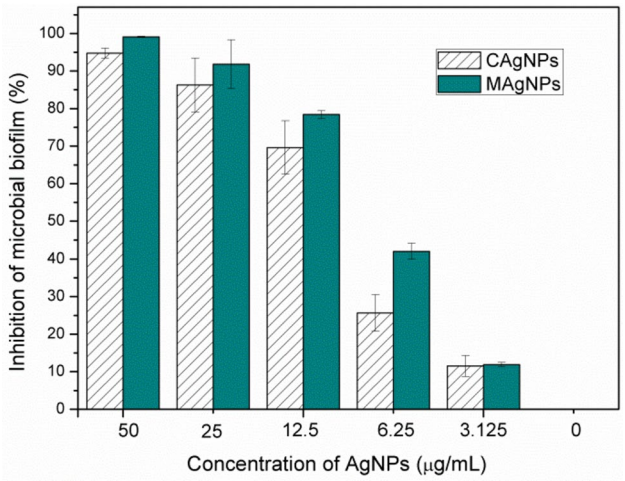

Fig. 4 Antibiofilm activity of CAgNPs and MAgNPs expressed as (%) inhibition, *n* = 3

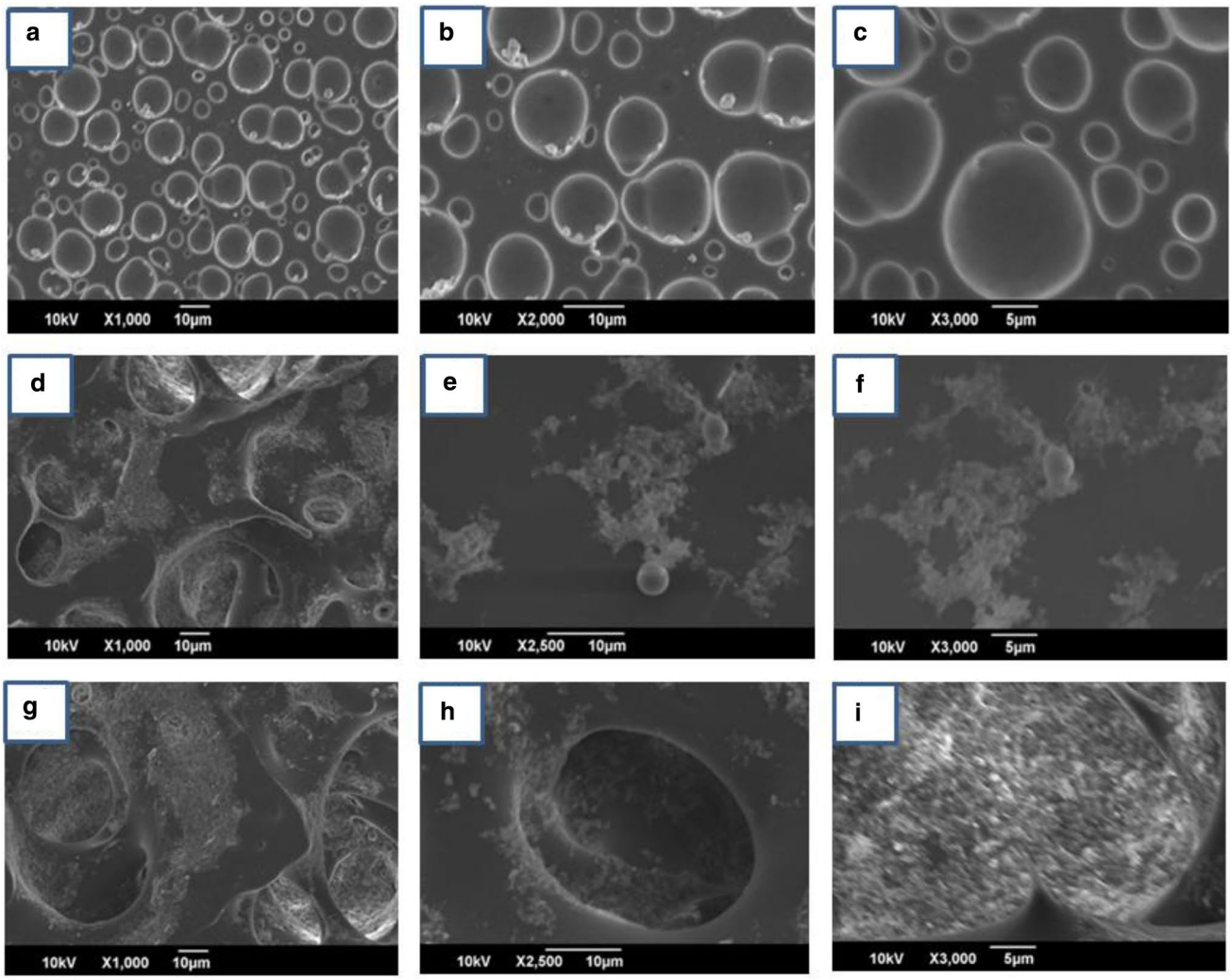

Fig. 5 Scanning electron micrograph of the surface of neat PMMA membrane (**a**–**c**) PMMA with CAgNPs (**d**–**f**) and PMMA with MAgNPs (**g**–**i**)

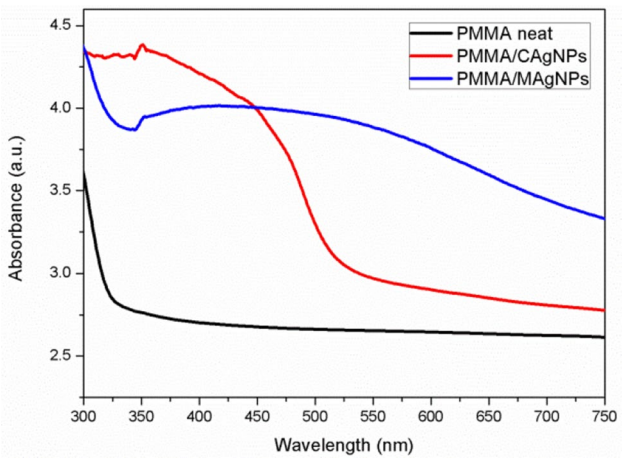

Fig. 6 UV–Vis spectra of PMMA, PMMA/CAgNP and PMMA/MAgNP nanocomposite membranes

TEM results of biofabricated AgNPs confirmed its nanoscale size. Also, the SPR peaks, characteristic of AgNPs could be clearly observed for both MAgNPs and CAgNPs. Since the same has been described as confirmatory to AgNPs in many previous studies, the presence of AgNPs in both the preparations could be confirmed (Thomas et al. 2012, 2015). The TEM micrographs of MAgNPs showed increased aggregation when compared to CAgNPs. Here, the particle size of the CAgNPs also appeared to be larger than that of MAgNPs.

The MIC and MBC analysis results also showed differences in activities of MAgNPs and CAgNPs. The MAgNPs were found to be more potent than CAgNPs because only about half the amount of MAgNPs was required to inhibit and kill *S. mutans* when compared to the CAgNPs. This could be attributed to the increased surface area of the MAgNPs due to its smaller size than CAgNPs. Here,

Fig. 7 Disc diffusion assay against *Streptococcus mutans* of (1) neat PMMA membrane (2) PMMA with CAgNPs (3) PMMA with MAgNPs

the small size of MAgNPs might also have favored its enhanced penetration into cells to affect the cellular components and thereby the viability of *S. mutans* (Shrivastava et al. 2007). Upon studying the antibiofilm properties of the NPs, MAgNPs inhibited the biofilm formation better than the CAgNPs. At 50 µg/mL concentration, MAgNPs was found to completely eliminate the formation of microbial biofilm as evidenced from spectrometry studies.

The surface morphology of nanocomposites prepared using PMMA and two kinds of AgNPs were examined by SEM. Neat PMMA membrane exhibited solvent evaporation induced smooth blind pores all over the surface. The low boiling point of used solvent might have resulted in rapid evaporation and thereby the appearance of pores in the thin films (Qian et al. 2010). The addition of the filler resulted in larger pores surrounded by white aggregates, which could be the added AgNPs. Upon filler addition, the boiling point of the solution might have increased to result in low evaporation rate and thereby larger but less number of pores. By the complete evaporation of the solvent, it might have favored the nanoparticles to assemble into the walls of micron sized pores. The MAgNPs, that appeared to be present along the pores of PMMA, could be due to its characteristic hydrophobic nature. However, majority of the CAgNPs were found to be accumulated in the cavity of the pores which points to the slight hydrophilic nature of these nanoparticles (Qian et al. 2010). From the UV–Vis spectra of the nanocomposite, the characteristic SPR peak of the MAgNPs and CAgNPs in PMMA appear to have broadened. This could be due to decrease in surface plasmon resonance absorbance of the nanoparticles in the PMMA matrix (Mei et al. 2014).

The PMMA/MAgNPs membrane exhibited a promising zone of clearance in the disc diffusion assay, but PMMA/CAgNPs showed no activity. The lack of activity of the CAgNPs incorporated membrane could be attributed to the presence of remnant of the curcuma extract as observed in the TEM micrographs (Fig. 3). These remnants seem to have interfered the activity of silver nanoparticles. In addition to this, earlier studies also suggested high levels of interactions between the PMMA and curcumin due to the presence of large number of hydroxyl groups in these two moieties (Balakrishnan et al. 2013). Such type of higher interaction between the PMMA and extract remnants seems to have a confinement effect on the Ag^+ ions, resulting in no visible microbicidal activity in the PMMA matrix.

Biofilm formation on the dental surface both on tooth and dental filling is a major concern nowadays. Both PMMA/AgNPs and PMMA/CAgNPs exhibited excellent antibiofilm properties as evidenced from the SEM micrographs (Fig. 8). The PMMA/CAgNPs exhibited strong antibiofilm properties but it did not show any antimicrobial property against *S. mutans*. Phytochemicals such as curcumin has been demonstrated to eradicate biofilms by interfering with the quorum sensing signaling systems (Loo et al. 2015; Méndez-Vilas 2011). The TEM micrographs (Fig. 3) of CAgNPs also showed the association of remnants of the extract with the formed AgNPs. Therefore, these moieties could also have contributed to the inhibition of microbial biofilms.

The microbially synthesized AgNPs have already been suggested to be more efficient and safer than the chemically synthesized AgNPs (Antony et al. 2011; Saifuddin et al. 2009). The potency and effectiveness of MAgNPs when compared to CAgNPs against microorganisms has been shown to be mechanistically different (Thomas et al. 2017). In a polymer matrix also, the MAgNPs exhibited excellent antimicrobial and antibiofilm properties asserting its effectiveness for dental application.

Conclusion

From the current study, the AgNPs synthesized using *B. amyloliquefaciens* SJ14 can be suggested to have superior antimicrobial and antibiofilm activities when compared to those synthesized using *C. aromatica* extract. The antimicrobial activity of the MAgNPs was more pronounced both alone as well as in the PMMA matrix. Thus, it can have promise as effective filler for the next generation of dental adhesive materials. The applications of AgNPs of microbial origin can be further extended to other medical device coatings, films, and household amenities which require strong and safe bactericidal surface.

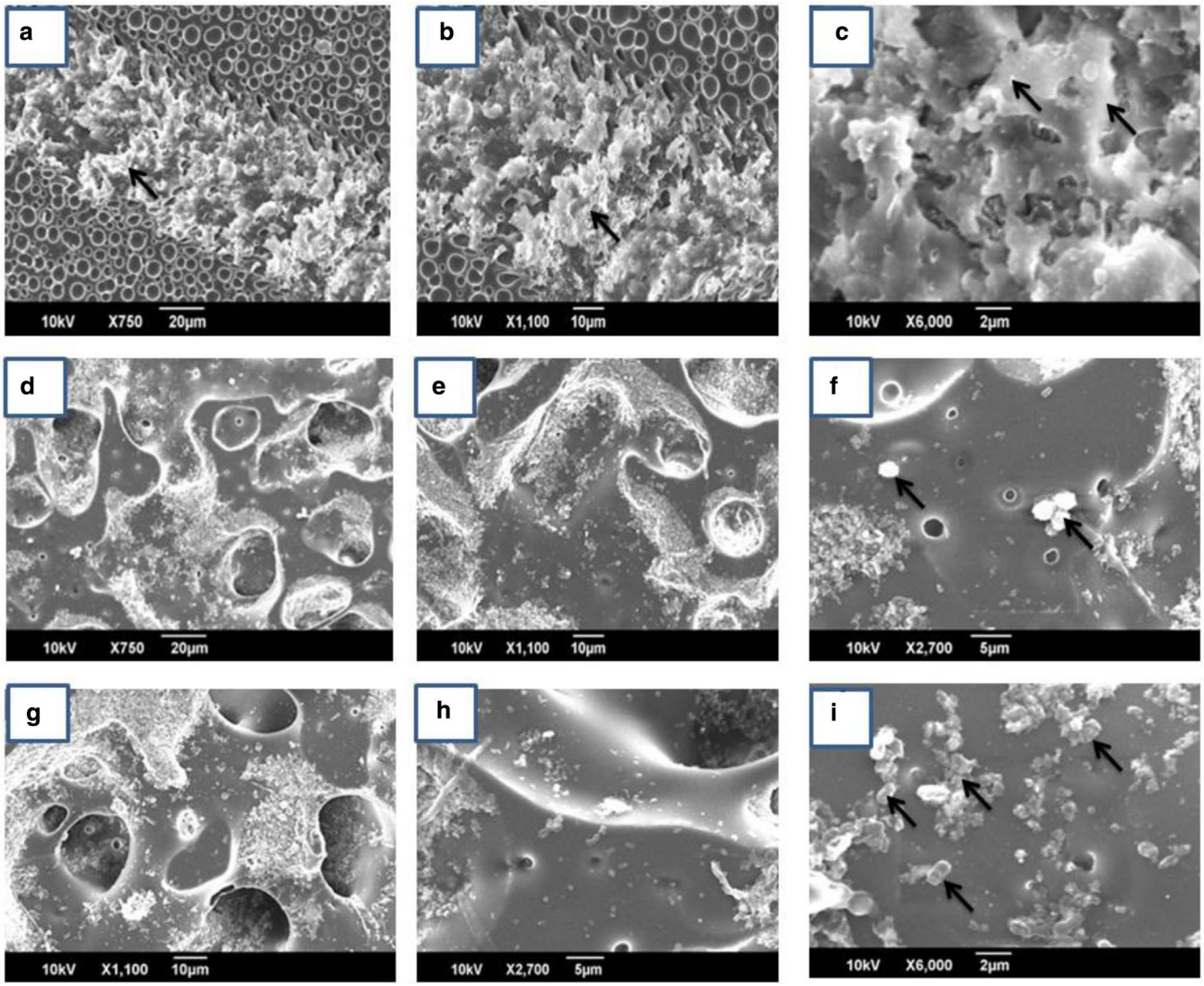

Fig. 8 Scanning electron micrographs of biofilm formed by *Streptococcus mutans* on nanocomposite membranes. Strong biofilm formation on PMMA membrane at different magnifications (**a**–**c**), inhibition of biofilm on PMMA/CAgNPs membrane (arrows indicate the biofilm formed on the thin film surface) (**d**–**f**) and inhibition in biofilm formation on PMMA/MAgNPs membrane (**g**–**i**). The arrows in figures **f** and **i** indicate isolated bacteria present in the nanocomposite thin films

Acknowledgements The authors gratefully acknowledge Indian Council of Medical Research (ICMR), New Delhi for the funded project on CoNS and Senior Research Fellowship to the author Roshmi Thomas. We also thank DBT-MSUB-IPLSARE programme in School of Biosciences, DST-Nanomission, International and InterUniversity Centre for Nanoscience and Nanotechnology, Mahatma Gandhi University for the help of UV–Vis Spectroscopy, FTIR, and HR-TEM analysis.

Compliance with ethical standards

Conflict of interest The authors declare that they have no conflict of interest.

References

Agarwala M, Choudhury B, Yadav RNS (2014) Comparative study of antibiofilm activity of copper oxide and iron oxide nanoparticles against multidrug resistant biofilm forming uropathogens. Indian J Microbiol 54(3):365–368

Antony JJ, Sivalingam P, Siva D, Kamalakkannan S, Anbarasu K, Sukirtha R, Krishnan M, Achiraman S (2011) Comparative evaluation of antibacterial activity of silver nanoparticles synthesized using Rhizophora apiculata and glucose. Colloids Surf B 88(1):134–140

Araruna FB, Quelemes PV, de Faria BEF, Kuckelhaus SAS, Marangoni VS, Zucolotto V, da Silva DA, Júnior JRS, Leite JRS, Eiras C (2013) Green synthesis and characterization of silver nanoparticles reduced and stabilized by Cashew Tree Gum. Adv Sci Eng Med 5(8):890–893

Babu SS, Augustine A, Kalarikkal N, Thomas S (2016) Nylon 6, 12/cloisite 30B electrospun nanocomposites for dental applications. J Siberian Federal Univ Biol 9(2):198

Balakrishnan VV, Abidin Z, Naziron N, Nasir K, Rusli M, Lee S, Kufian M, Majid S, Vengadaesvaran B, Arof A (2013) Influence of curcumin natural dye colorant with PMMA-acrylic polyol blended polymer. Pigm Resin Technol 42(2):95–102

Christensen GD, Simpson W, Younger J, Baddour L, Barrett F, Melton D, Beachey E (1985) Adherence of coagulase-negative staphylococci to plastic tissue culture plates: a quantitative model for the adherence of staphylococci to medical devices. J Clin Microbiol 22(6):996–1006

Clement JL, Jarrett PS (1994) Antibacterial silver. Met Based Drugs 1(5–6):467–482

Das VL, Thomas R, Varghese RT, Soniya E, Mathew J, Radhakrishnan E (2014) Extracellular synthesis of silver nanoparticles by the Bacillus strain CS 11 isolated from industrialized area. 3 Biotech 4(2):121–126

Dias HB, da Silva Souza VTF, Martins RA, Mendes ACB, de Souza MIAV, Zuanon ÂCC, de Souza Rastelli AN (2017) Functional dental restorative materials that hinder oral biofilm. Curr Oral Health Rep 4(1):22–28

Dionysopoulos D, Tolidis K, Gerasimou P, Papadopoulos C (2017) Effect of filler composition of dental composite restorative materials on radiopacity in digital radiographic images. Polym Compos 39:E351–E357

Elshikh M, Ahmed S, Funston S, Dunlop P, McGaw M, Marchant R, Banat IM (2016) Resazurin-based 96-well plate microdilution method for the determination of minimum inhibitory concentration of biosurfactants. Biotechnol Lett 38(6):1015–1019

Frazer RQ, Byron RT, Osborne PB, West KP (2005) PMMA: an essential material in medicine and dentistry. J Long Term Effects Med Implants 15(6):629–639

Garcia S, Blackledge M, Michalek S, Su L, Ptacek T, Eipers P, Morrow C, Lefkowitz E, Melander C, Wu H (2017) Targeting of *Streptococcus mutans* biofilms by a novel small molecule prevents dental caries and preserves the oral microbiome. J Dental Res 96(7):807–814

Ge L, Li Q, Wang M, Ouyang J, Li X, Xing MM (2014) Nanosilver particles in medical applications: synthesis, performance, and toxicity. Int J Nanomed 9:2399

Lee J-H, Jo J-K, Kim D-A, Patel KD, Kim H-W, Lee H-H (2018) Nano-graphene oxide incorporated into PMMA resin to prevent microbial adhesion. Dent Mater 34(4):e63–e72

Loesche WJ (1986) Role of *Streptococcus mutans* in human dental decay. Microbiol Rev 50(4):353

Loo C-Y, Rohanizadeh R, Young PM, Traini D, Cavaliere R, Whitchurch CB, Lee W-H (2015) Combination of silver nanoparticles and curcumin nanoparticles for enhanced anti-biofilm activities. J Agric Food Chem 64(12):2513–2522

Marashdeh MQ, Gitalis R, Levesque C, Finer Y (2018) Enterococcus faecalis hydrolyzes dental resin composites and adhesives. J Endod 44(4):609–613

Mathew S, Snigdha S, Mathew J, Radhakrishnan E (2018) Poly (vinyl alcohol): montmorillonite: boiled rice water (starch) blend film reinforced with silver nanoparticles; characterization and antibacterial properties. Appl Clay Sci 161:464–473

Mei L, Lu Z, Zhang X, Li C, Jia Y (2014) Polymer-Ag nanocomposites with enhanced antimicrobial activity against bacterial infection. ACS Appl Mater Interf 6(18):15813–15821

Méndez-Vilas A (2011) Science and technology against microbial pathogens: research, development and evaluation: proceedings of the international conference on antimicrobial research (ICAR2010), Valladolid, Spain, 3–5 Nov 2010. World Scientific

Parikh RY, Singh S, Prasad B, Patole MS, Sastry M, Shouche YS (2008) Extracellular synthesis of crystalline silver nanoparticles and molecular evidence of silver resistance from *Morganella* sp.: towards understanding biochemical synthesis mechanism. ChemBioChem 9(9):1415–1422

Parikh RY, Ramanathan R, Coloe PJ, Bhargava SK, Patole MS, Shouche YS, Bansal V (2011) Genus-wide physicochemical evidence of extracellular crystalline silver nanoparticles biosynthesis by *Morganella* spp. PLoS One 6(6):e21401

Peters A, Arnold C, Setz JM, Boeckler AF (2010) Factors in polymerization influencing the accuracy of PMMA denture bases. Int Poster J Dent Oral Med12(1):Poster 476

Qian Y-F, Su Y, Li X-Q, Wang H-S, He C-L (2010) Electrospinning of polymethyl methacrylate nanofibres in different solvents. Iran Polym J 19(2):123

Quaresma P, Soares L, Contar L, Miranda A, Osório I, Carvalho PA, Franco R, Pereira E (2009) Green photocatalytic synthesis of stable Au and Ag nanoparticles. Green Chem 11(11):1889–1893

Saifuddin N, Wong C, Yasumira A (2009) Rapid biosynthesis of silver nanoparticles using culture supernatant of bacteria with microwave irradiation. J Chem 6(1):61–70

Saini R, Saini S, Sharma S (2011) Biofilm: a dental microbial infection. J Nat Sci Biol Med 2(1):71–75. https://doi.org/10.4103/0976-9668.82317

Shameli K, Ahmad MB, Zamanian A, Sangpour P, Shabanzadeh P, Abdollahi Y, Zargar M (2012) Green biosynthesis of silver nanoparticles using Curcuma longa tuber powder. Int J Nanomed 7:5603

Shrivastava S, Bera T, Roy A, Singh G, Ramachandrarao P, Dash D (2007) Characterization of enhanced antibacterial effects of novel silver nanoparticles. Nanotechnology 18(22):225103

Srivastava M, Singh S, Self WT (2012) Exposure to silver nanoparticles inhibits selenoprotein synthesis and the activity of thioredoxin reductase. Environ Health Perspect 120(1):56

Takeyama M, Kashibuchi S, Nakabayashi N, Masuhara E (1978) Studies on dental self-curing resins (17). Adhesion of PMMA with bovine enamel or dental alloys (author's transl). Shika rikogaku zasshi J Jpn Soc Dental Apparatus Mater 19(47):179–185

Thomas R, Jasim B, Mathew J, Radhakrishnan E (2012) Extracellular synthesis of silver nanoparticles by endophytic *Bordetella* sp. isolated from *Piper nigrum* and its antibacterial activity analysis. Nano Biomed Eng 4(4):183–187

Thomas R, Soumya K, Mathew J, Radhakrishnan E (2015) Electrospun polycaprolactone membrane incorporated with biosynthesized silver nanoparticles as effective wound dressing material. Appl Biochem Biotechnol 176(8):2213–2224

Thomas R, Mathew S, Nayana A, Mathews J, Radhakrishnan E (2017) Microbially and phytofabricated AgNPs with different mode of bactericidal action were identified to have comparable potential for surface fabrication of central venous catheters to combat Staphylococcus aureus biofilm. J Photochem Photobiol B Biol 171:96–103

Velmurugan P, Anbalagan K, Manosathyadevan M, Lee K-J, Cho M, Lee S-M, Park J-H, Oh S-G, Bang K-S, Oh B-T (2014) Green synthesis of silver and gold nanoparticles using Zingiber officinale root extract and antibacterial activity of silver nanoparticles against food pathogens. Bioprocess Biosyst Eng 37(10):1935–1943